Physical Modeling of Liquid/Liquid Mass Transfer in Gas Stirred Ladles

SEON-HYO KIM and R. J. FRUEHAN

Several of the metallurgical reactions occurring in gas stirred steel ladles are controlled by liquid phase mass transfer between the metal and slag. In order to calculate the rate of these reactions, information about the two phase mass transfer parameter is necessary. The mass transfer between two immiscible liquids, oil and water simulating slag and steel, respectively, was measured in a scale model of a ladle. The mass transferred species was thymol which has an equilibrium partition ratio between oil and water similar to that for sulfur between slag and metal. The mass transfer rate was measured as a function of gas flow rate, tuyere position and size, method of injection, oil viscosity, and oil/water volume ratio. In addition, mixing times in the presence of the oil layer and mass transfer coefficient for the dissolution of solid benzoic acid rods were measured. The results show that there are three gas flow rate regimes in which the dependence of mass transfer on gas flow rate is different. At a critical gas flow rate, the oil layer breaks into droplets which are entrained into the water, resulting in an increase in the two phase interfacial area. This critical gas flow rate was found to be a function of tuyere position, oil volume, densities of two phases, and interfacial tension. Two phase mass transfer for a lance and a tuyere was found to be the same for the same stirring energy in low energy regions regardless of lance depth. Mass transfer is faster for a center tuyere as compared to an offcenter tuyere, but mixing times are smaller for the offcenter tuyere. From the results obtained, the optimum stirring conditions for metallurgical reactions are qualitatively discussed.

I. INTRODUCTION

DUE to the need for cleaner steels and higher productivity, secondary refining or ladle metallurgy has grown dramatically in the past few years. The ladle metallurgical processes can vary from simple addition of a synthetic slag into the ladle followed by argon bubbling to highly sophisticated arc heated ladle systems equipped with vacuum, powder injection, argon bubbling, and in some cases induction stirring for inclusion removal, desulfurization, dephosphorization, and alloying. The advantages of ladle refining by gas stirring are that its capital cost is low, it enhances inclusion flotation, and it gives good refining efficiency by leading to a faster approach to equilibrium because of a better mass transfer rate between slag and metal. In a gas stirred ladle, bubbles rising through the liquid induce a recirculatory flow of fluid because of the reduced density in a gas/liquid plume. Bubbles may also cause the ejection of small droplets of one phase into the other.

Much of the previous work[1-10] on physical and mathematical modeling of gas stirred ladles was concerned with fluid flow and mixing times in the metal. However, the rate-controlling process for most metallurgical reactions such as desulfurization is two phase mass transfer between slag and metal, not one phase mixing as represented by mixing times.

The mixing of liquids in metallurgical vessels has been studied to relate the mixing time (τ_m) with mixing power density (ε).[11-15,27] The mixing time was defined as the time corresponding to the arbitrary level of approach to the final steady state concentration. Empirical relationships of the type $\tau_m \propto \varepsilon^n$ have been proposed, and various values of n have been reported. Asai *et al.*[11] and Mazumdar[13] have analyzed theoretically and experimentally these relationships and confirmed their theoretical results by carrying out water model experiments. In separate studies, they agreed that τ_m is proportional to $\varepsilon^{-1/3}$ and is dependent on the vessel size in a flow regime predominated by turbulent viscous force. Mazumdar further related the mixing times in the model ladle ($\tau_{m,\text{model}}$) to those in full scale systems ($\tau_{m,\text{f.s.}}$) through the geometrical scaling factor for axisymmetrically gas agitated systems using the relationship:

$$\tau_{m,\text{model}} = \tau_{m,\text{f.s.}} \cdot \lambda^{3/4}$$

The effect of the presence of a slag layer in gas stirred ladles on the mixing time was investigated by Haida *et al.*[14] and Ying *et al.*[15] In these respective works, they showed that mixing time increases with the presence of slag and the absolute value of exponent (n) is generally higher than that obtained without the slag present. The interaction between mixing time and mass transfer rate has not been mentioned clearly until now. Very recently, Matway[24] asserted that the mass transfer increases as the mixing time decreases for specific circumstances in his study of a BOF scale model using various tuyere patterns.

In a gas stirred ladle, the turbulence caused by a gas/liquid plume rising through the bath in the upper portion of the vessel and the recirculating motion in the bath facilitate the metallurgical reactions at the interface between two immiscible liquid phases by giving high mass transfer rates. The product of the mass transfer coefficient and the interfacial area, kA (mass transfer parameter), is the only parameter measured in the experiments of liquid phase mass transfer because of difficulty in measuring the interfacial area between the slag and metal. Due to the slag/metal mixing, the area is generally greater than the planar area

SEON-HYO KIM, formerly Graduate Student in the Department of Metallurgical Engineering and Materials Science, Carnegie Mellon University, is Assistant Professor with the Department of Metallurgy and Materials Science, Pohang Institute of Science and Technology, Pohang, Kyungbuk, Korea. R. J. FRUEHAN, Professor, is with the Department of Metallurgical Engineering and Materials Science, Carnegie Mellon University, 5000 Forbes Avenue, Pittsburgh, PA 15213.

Manuscript submitted May 12, 1986.

between the two phases. Asai *et al.*[9] comprehensively reviewed the previous work concerning the effect of gas flow rate on the mass transfer rate between two immiscible liquids, and showed that the results of previous work as well as their own water modeling work in terms of the values of exponent (n) in the relation of $K \propto Q^n$. Numerous values[16–24] of n, depending on the systems of two immiscible phases and the operating variables of the system, have been reported. It is interesting to note that the results of desulfurization of steel by a synthetic slag in a plant scale ladle show an abrupt increase of the value of the exponent from 0.25 to 2.1, and from 0.3 to 1.3 at a critical gas flow rate.[21,22] This abrupt change was partially explained by the authors[21,22] as being due to the change of mixing pattern and as an effect of the increased heating of the slag layer at higher gas flow rates by the others.[9] The existence of such an abrupt transition of the mass transfer rate in two immiscible liquid systems has also been observed in many water model studies investigating the transfer of some organic species between two immiscible liquids.[16–20,23,24] Based on the previous results of both high temperature experiments and cold model experiments, there appear to be at least two or possibly more physical regimes of gas flow, where different values of n apply depending on the operating system variables.

Despite many previous studies done on liquid/liquid mass transfer in gas stirred vessels, questions still exist concerning the optimum stirring conditions for better liquid phase mass transfer; *e.g.*, location of plugs, number of plugs, gas flow rate, and other system variables. It is the purpose of this study to investigate the dependence of the mass transfer parameter on the operating system variables such as gas flow rate, number and position of tuyeres, lance injection, volume ratio of two immiscible liquids, and physical properties of liquids. The effect of the presence of a secondary immiscible liquid and tuyere location on mixing times are also investigated. In addition, mass transfer between a solid rod of known surface area and the liquid was examined to approximately separate the mass transfer coefficient term from the mass transfer parameter obtained in liquid/liquid system. In a future publication, the results of this study will be explained by a dimensional analysis of the system.

II. EXPERIMENTAL TECHNIQUE AND MASS TRANSFER EQUATIONS

A scale model of a steelmaking ladle (1/7.2 scale of a 200 ton steel ladle) with a bottom diameter of 45.6 cm, a 10 pct taper (2.5 deg), and a height of 62 cm was used. The liquid was usually filled to a height of 44.5 cm. The system has four positions for tuyeres: one at the center, one each at one-half the radius, and one at the bottom of vessel side wall. The air flow rate was monitored by rotameters on each gas line leading to a tuyere, which had a diameter of 0.2 or 0.48 cm. The model lance was a stainless steel tube with side holes or ports (0.48 cm in diameter) at the tip.

The modified Froude number (N'_{Fr}), defined as the ratio of two times the kinetic energy of the gas injected through a tuyere to the buoyancy energy of the gas, was considered as the similarity criterion to correlate the gas flow rate between the scale model and full scale system.

$$N'_{Fr} = \frac{\rho_g U_T^2}{\rho_l g L} \qquad [1]$$

The linear gas velocity at the exit of a tuyere is expressed in terms of a gas flow rate and tuyere diameter as follows:

$$\rho_g U_T = \frac{Q}{22.4}\frac{M}{60}\frac{1}{\pi d_T^2/4} \qquad [2]$$

where M is a molecular weight of the gas (grams), and d_T is a diameter of the tuyere (cm).
Then,

$$N'_{Fr} = \frac{(\rho_g U_T)^2}{\rho_l \rho_g g L} = C\frac{Q^2}{L d_T^4} \qquad [3]$$

where

$$C = \frac{9.159 \times 10^{-10} M^2}{\rho_l \rho_g}$$

Applying a modified Froude criterion between the model and full scale system, one finds:

$$(N'_{Fr})_{model} = (N'_{Fr})_{full\ scale} \qquad [4]$$

Then,

$$Q_{f.s.} = \left(\frac{C_m}{C_{f.s.}}\right)^{1/2} \lambda^{5/2} Q_m \qquad [5]$$

where λ is a geometrical scale factor (a ratio of characteristic lengths of systems ($L_{f.s.}/L_m$)). If one applies this correlation to the systems of steel/Ar and water/air, then

$$Q_{f.s.} = 1.038\lambda^{5/2} Q_m \qquad [6]$$

Therefore, the scaled gas flow rate of 1 SCFM in a 200 ton steel ladle would be approximately equal to 0.2 l/min in this scale model system, assuming a modified Froude number criterion for the bulk fluid flow.

Measurements of the mixing times were carried out by injection of a tracer (80 ml of 2.5 N KCl solution) into the water bath (75 l) and by using a conventional electric conductance measurement method. The conductivity cell was immersed to a depth of 1 cm away from the bottom and near the wall of a model ladle. A tracer was injected into the water bath at the center of the plume eye on the bath surface. In order to avoid the additional mixing due to the kinetic energy of the tracer, experiments were done by gently pouring the tracer onto the bath surface. The change of conductivity in the water with the time was measured. The mixing time is defined as the time in which the tracer concentration in the water falls within ±5 pct of the steady state concentration. 2.5 l of oil was covered on the top to investigate the effect of slag layer on the mixing phenomena.

For mass transfer between two immiscible liquids, there are two liquid phase boundary layers offering resistances to overall mass transfer. The overall mass transfer coefficient at the interface can be calculated by equating the mass fluxes at the two phase boundaries under steady state condition.

$$J = k_m(C_m - C'_m) = k_s(C'_s - C_s) \qquad [7]$$

Considering an equilibrium at the interface gives the following equation:

$$h = \frac{C'_s}{C'_m} \qquad [8]$$

Combining the above equations gives

$$C'_m = \frac{k_m C_m + k_s C_s}{k_m + h k_s} \qquad [9]$$

After substituting the above equation into the flux equation for the metal phase, the flux equation reduces to

$$J = \frac{C_m - C_s/h}{1/k_m + 1/(hk_s)} = K_o\left(C_m - \frac{C_s}{h}\right) \quad [10]$$

where K_o is the overall mass transfer coefficient.

$$K_o = \frac{1}{1/k_m + 1/(hk_s)} \quad [11]$$

In this equation, $1/k_m$ and $1/(hk_s)$ represent the resistances to mass transfer in the metal and slag phases, respectively. It is generally acknowledged that the difference between k_m and k_s may be assumed to be within an order of magnitude. Accordingly, depending on the value of h in a specific system, the resistance in one phase boundary layer can be so great as to make the resistance of the other phase boundary layer insignificant, or both the phase resistances can affect significantly the mass transfer rate.

In several previous studies of mass transfer in liquid/liquid systems, β-naphthol ($C_{10}H_8O$) was used as the transferring tracer, paraffin oil as the slag phase, and water as the steel phase. However, β-naphthol has a partition ratio, h, between oil and water of less than one (0.6). This leads to liquid phase mass transfer being controlled by mass transfer in the oil phase. The transfer of a tracer from oil phase to the water phase was investigated in all previous mass transfer studies using a cold model. These are not the modeling conditions in real systems such as sulfur transfer from metal to slag. The partition ratio of sulfur between slag and metal is on the order of 200 to 500, resulting in the liquid phase mass transfer controlled by metal phase resistance. Therefore, an ideal cold model system using thymol ($C_{10}H_{14}O$) as a tracer and a 50/50 mixture (by volume) of paraffin oil and cottonseed oil as the slag phase developed recently by Matway,[24] was adopted because the partition ratio of thymol in this system is high (>350). The transfer of a tracer from water to oil phase was investigated in this study.

Typically, 75 l of water containing 120 to 130 ppm thymol was placed in the ladle model followed, in most cases, by placing 2.5 l of oil on top. This is the approximate steel to slag volume ratio used in actual practices (normally the slag to metal ratio in ladle treatment is less than 0.1).[25] After gas stirring is started, samples are taken out of the water as a function of time and in some cases as a function of position in the ladle. The samples were allowed to settle for several hours to float up the oil sampled with water, then were carefully treated using a pipet to remove the oily surface, and finally filtered using filter papers to obtain clean water samples. The samples were analyzed by a UV-spectrophotometer to determine the concentration of the transferred species in water.

The mass transfer equations for the model system are the same as for a real system. The mass transfer equation in the case of liquid phase mass transfer due to the resistance of the water phase boundary layer can be expressed as:

$$\frac{dC_w}{dt} = \frac{k_w A}{V_w}(C_w - C_w') \quad [12]$$

$$h = \frac{C_w'}{C_o} \quad [13]$$

The mass balance for the transferred species is

$$(C_w^\circ - C_w)V_w = C_o V_o \quad [14]$$

Assuming equilibrium at the interface, the combinations of the above equations reduce to

$$\int_{C_w^\circ}^{C_w} \frac{dC_w}{(1 + hV_w/V_o)C_w - hC_w^\circ V_w/V_o} = \frac{k_w A}{V_w}\int_0^t dt \quad [15]$$

Integration of the above equation yields the following form of mass transfer equation for a constant partition ratio:

$$\frac{\ln[(1 + hV_w/V_o)C_w/C_w^\circ - hV_w/V_o]}{1 + hV_w/V_o} = \frac{k_w A}{V_w}t \quad [16]$$

In this investigation, the left-hand side is referred to as LHS. Plotting LHS *vs* time for each experimental result should give a straight line with a slope equal to $k_w A/V_w$.

When the gas is injected into the bath, a "plume eye" develops where the oil layer is pushed open by the gas. The size of the plume eye was measured as a function of flow conditions to determine the planar interfacial area of oil and water.

For the mass transfer study between solid rods and water, samples were prepared by melting benzoic acid powder and casting it into a cylindrical shape with a wire inserted in the center. To ensure an equal amount of exposed surface area on each sample, paraffin wax was used to coat the end of the sample that has the holding wire extending from it. About 2 cm of exposed benzoic acid remains on each sample after preparation. The benzoic acid rod sample was attached to a rod that holds it securely during each experimental trial and placed in the water bath at various positions. The experimental time was 20 minutes to allow for adequate weight loss. After each experiment, the weight loss was measured and used to calculate the mass transfer coefficient.

The mass transfer equation for the calculation of a mean mass transfer coefficient in the dissolution of the solid rod into the liquid, can be expressed by

$$\frac{dW}{dt} = k_w A(C_i - C_b) \quad [17]$$

The following assumptions are made to simplify the mass transfer equation:

1. The driving force is constant during the dissolution test.
2. The surface area is equal to the arithmetic mean area $[\bar{A} = 0.5(A_{\text{initial}} + A_{\text{final}})]$.
3. The mass transfer coefficient (k_w) corresponds to a mean value ($\bar{k}_w$) for the entire surface of the exposed area disregarding the peripheral and planar distribution of the mass transfer coefficient around the cylindrical rod.

The above equation is simplified as:

$$\bar{k}_w = \frac{\Delta W}{C_i \bar{A}\,\Delta t} \quad [18]$$

III. RESULTS AND DISCUSSION

A. *Effect of Second Phase on Mixing Time*

Figure 1 shows a plot of mixing times as a function of gas flow rate for a center, an offcenter, and a side tuyere with an oil layer present. All the mixing time results, measured

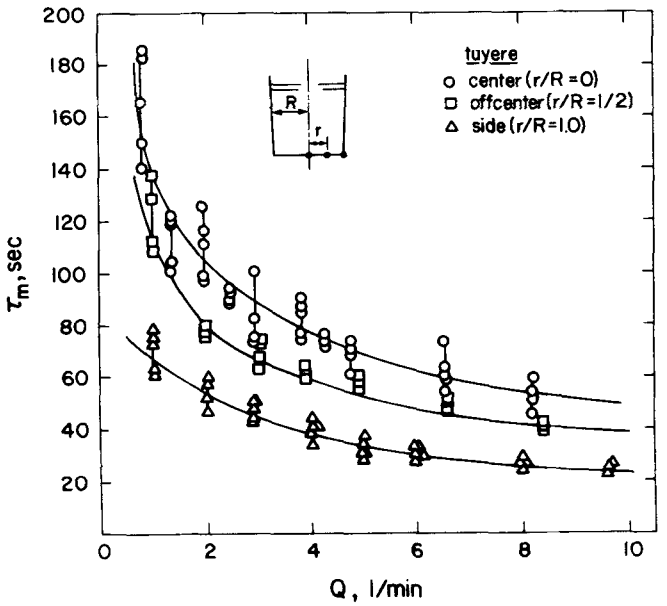

Fig. 1—A plot of mixing time as a function of gas flow rate for three different arrangements of a tuyere with an oil layer present.

4 to 6 times for each gas flow rate, are shown. It is interesting to note that shorter mixing times are observed as the position of a single tuyere moves from the center toward the wall of a vessel. As the tuyere position becomes more offcentered, the mixing of the wall side regions closer to the gas/liquid plume occurs more quickly than the other regions away from the gas/liquid plume. Therefore, the effect of mixing in one wall side region on the mixing in the other wall side region (mixing phenomena due to eddy diffusion inside the gas/liquid plume) becomes less significant as the tuyere position becomes more offcentered. This explanation is supported by visual observation using a dye tracer in place of the KCl solution. Asai *et al.*[11] explained this phenomenon by describing that increase of fluid circulatory loop in a vessel tends to decrease mixing time.

Plotting of mixing time in terms of stirring energy density (ε) is depicted in Figure 2 to compare the present experimental results with those of other theoretical and experimental studies. The present mixing time results with and without an oil layer are plotted together to demonstrate the effect of the oil layer on the mixing time distribution. Stirring energy density is calculated by considering the potential energy increase due to the isobaric expansion at the tuyere exit and isothermal expansion during the rise of bubbles.

$$\varepsilon = \frac{0.01425QT \log(1 + H/1033.9)}{W_b} \quad [19]$$

The presence of an oil layer increases the mixing time significantly regardless of injection patterns as shown in Figure 2. Similar results have been reported but without detailed explanations.[14,15] In the presence of the oil layer, some of the stirring energy by gas injection is consumed in producing a turbulence at the interfacial region and a circulation inside the oil. Therefore, less energy is used for the mixing phenomenon inside the bulk phase. This effect implies the resistance of an oil layer to the recirculatory velocity of bulk fluid. This finding also indicates the weakness of the existing mathematical models to describe the velocity profile in the bulk phase, which was developed without considering the effect of secondary phase (slag layer). The slope of the lines, n, in Figure 2 without an oil layer for a center tuyere injection (-0.32) is in good agreement with the theoretical one (-0.33) derived by Lehner,[26] Asai *et al.*,[11] and Mazumdar.[13] Considering the experimental scatter, the value of n with an oil layer (-0.43) is also consistent with those determined from both plant scale experiments with a slag layer[27] and water modeling experiments using simulated slag.[14,15] In general, the absolute value of exponent n becomes larger with the presence of slag layer regardless of the operating system variables. The value of n for offcenter tuyeres is the same as that for a center tuyere injection experiment with an oil layer.

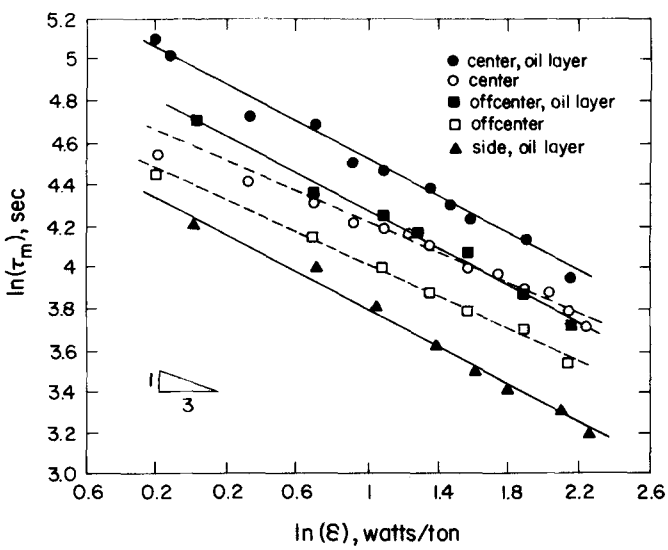

Fig. 2—Mixing time *vs* stirring energy density for 3 different tuyere patterns with and without an oil layer.

B. *Two Phase Mass Transfer*

The reaction rate of a slag/metal or any two phase reaction is significantly increased by gas stirring because of the faster replacement of the major heavier phase (metal) at the interface and the generation of additional interfacial area. Typical experimental data of liquid/liquid mass transfer are shown in Figure 3, where LHS of Eq. [16] is plotted as a function of time. This plot shows a linear relationship between the LHS and time and gives a slope of $k_w A/V_w$.

Effect of Gas Flow Rate: Figure 4 shows a plot of $k_w A$ as a function of gas flow rate for a center tuyere. The mass transfer parameter, $k_w A$, increases slowly with increasing flow rate for low flows. There is an abrupt increase of $k_w A$ at higher flow rates (>4.5 l/min). A different behavior of interaction between oil and water phases was visually observed with increasing flow rate. As shown in Figure 5, the ln-ln plot for $k_w A$ and flow rate, a center tuyere arrangement for stirring produces three regimes of flow rates in which the dependence of $k_w A$ on the gas flow rate is different. Regime I (low gas flow rate region) shows a 0.6 order dependence of $k_w A$ on Q. The mass transfer rate is a weak function of flow rate in this regime where the oil layer is very calm, no oil droplets are driven into the water, and the interface between oil and water phases is close to planar surface except for the very weak wave motion of the interface near the edge of plume eye. In Regime II of

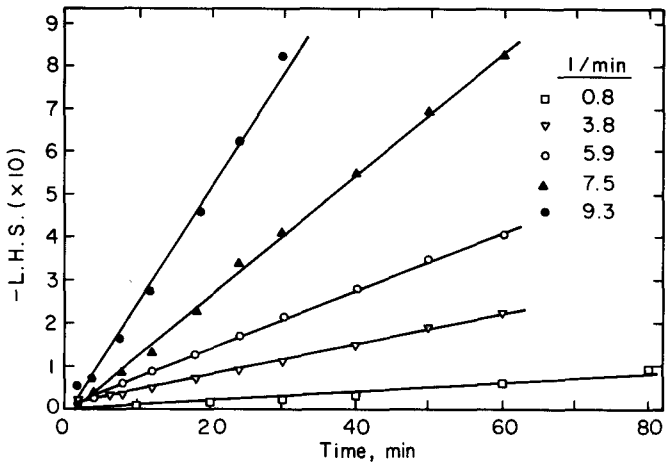

Fig. 3—Relationship between LHS of mass transfer Eq. [10] and time for center tuyere injection.

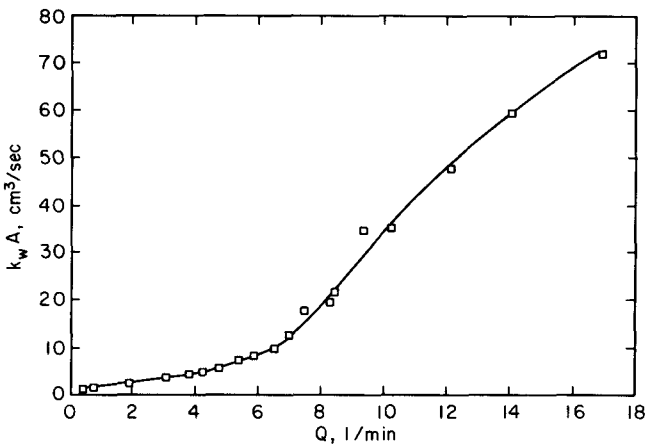

Fig. 4—A plot of k_wA as a function of gas flow rate for center tuyere injection.

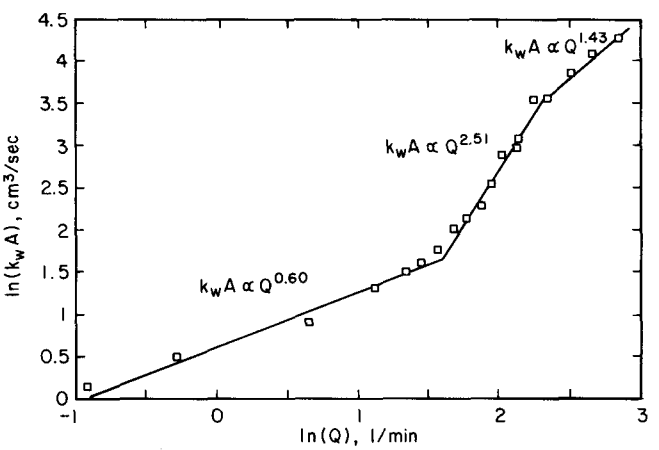

Fig. 5—Relationship between k_wA and flow rate in terms of the order dependence, n, for center tuyere injection.

intermediate flow rates (4.5 to 9 l/min), the exponent value of k_wA on Q is as high as 2.5. This high value and the abrupt change of the dependence can be explained by the observation that the oil layer near the edge of a plume eye continuously forms oil ligaments and then breaks up into droplets which are entrained into the water. This phenomenon increases the oil/water interfacial area. The critical gas flow rate defines the boundary between Regime I and Regime II. It is at this gas flow rate that oil droplets are formed and the entrainment of these droplets into the bulk liquid phase starts to occur. At higher gas flow rates (Regime III, $Q > 9.5$ l/min), k_wA is proportional to $Q^{1.43}$. At this higher gas flow rate region, nearly the entire oil layer breaks down into oil droplets without forming oil ligaments near the edge of plume eye right after gas injection, and the penetration of oil droplets deep into the water bath occurs. The effect of stronger agitation on the mass transfer rate begins to decrease because the size and number of oil droplets approach steady state. The recirculation and entraining depth of the oil droplets in the liquid bath are the major parameters increasing the mass transfer instead of the number of entrained oil droplets. Similar trends of the dependence of k_wA on Q were also observed in previous mass transfer studies in both water modeling systems[16–20,23,24] and commercial plant scale systems.[21,22]

Effect of Oil Viscosity: Experiments were carried out to determine the effect of oil viscosity on k_wA. The measured physical properties of a light paraffin oil mixture and a heavy paraffin oil mixture with cottonseed oil are shown in Table I. As shown in Figure 6, no difference in k_wA with different oils was observed in the low gas flow rate region. The starting gas flow rate for entraining oil droplets into water is the same in the high and low viscosity oils. However, k_wA for the high viscosity oil is slightly lower at high gas flow rates than that for low viscosity oil, because a greater number of oil droplets forms for lower viscosity oil. These results indicate that oil viscosity affects the mass transfer rate to some extent in the higher gas flow rate region where the oil droplet formation and entrainment into water

Table I. Physical Properties of Selected Materials

Type of Oil	Density (gr/cm³)	Viscosity (Poise)	Interfacial Tension with Water (dynes/cm)
light paraffin oil + cottonseed oil	0.886	0.334	18.12
heavy paraffin oil + cottonseed oil	0.896	0.475	19.38
light paraffin oil	0.850	0.323	41.84

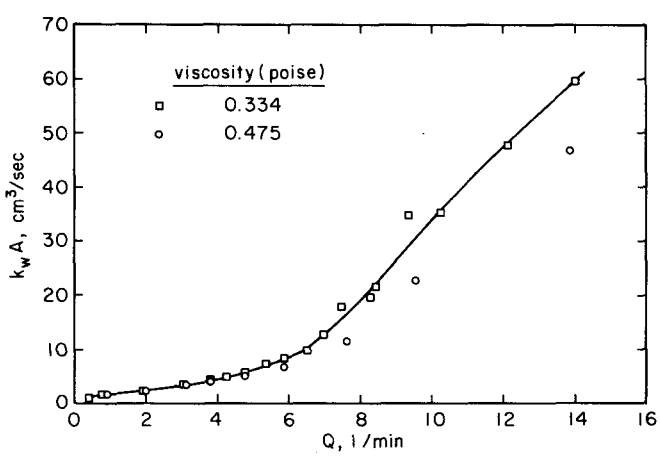

Fig. 6—Effect of oil viscosity on the mass transfer parameter for center tuyere injection.

occurs. It can be said that the critical gas flow rate is not a function of oil viscosity even though the oil viscosity changes the rate of oil droplet formation. This finding is in good agreement with the qualitative explanation based on visual observation by Billington *et al.*[28] His observation showed that the rate of droplet formation is constant in the low gas flow rates regardless of oil viscosities, but the rate of droplet formation of the lower viscosity oil increases more rapidly than that of the higher oil viscosity in the regime of higher gas flow rate. It was also reported that the equilibrium size of the largest oil droplets becomes larger and the mean diameter of oil droplets increases as the viscosity of the dispersed phase increases.[29] Therefore, the different size distribution of droplets according to the oil viscosity can also explain the slight difference of mass transfer in higher flow rates for two different viscosities of the oils.

Effect of Interfacial Tension: The interaction between the oil layer and water was visually studied to determine the effect of interfacial tension between two phases on the critical gas flow rate. The liquid/liquid systems of light paraffin oil/water and light paraffin oil plus cottonseed oil/water were used for this study mainly because of the close values of oil viscosities. The physical properties of these oils are shown in Table I. It was found that the critical gas flow rate for light paraffin oil/water system is higher than for the other system: 7 l/min for light paraffin oil/water system and 4.5 l/min for the other system, where the same ratio of oil to water (2.5 l/75 l) was used, respectively. The slight difference of densities between these oils can not change the critical gas flow rate significantly, even though it is a critical parameter for the determination of critical flow rate; the effect of density differences between two immiscible phases on the critical gas flow rate was preliminary studied and found to be very significant. This visualization result showed that the interfacial tension between two immiscible phases is an important parameter for the breakage and entrainment of the oil, and the critical gas flow rate increases with the higher interfacial tension of phases. Wang and Calabrese[30] reported that the relative influence of interfacial tension decreases as the dispersed-phase viscosity increases, and further proposed that the resistance to oil breakage due to interfacial tension becomes negligible relative to viscous resistance only at about $\mu_d > 10$ poise for systems of low interfacial tension. The present result agrees well with this observation since the viscosities of various oils in the present study are much smaller than 10 poise.

Effect of Oil Volume Fraction: Figure 7 shows the effect of the volume fraction of oil on k_wA. The larger amount of oil increases the mass transfer rate by the formation of oil droplets at slightly lower gas flow rates. For low gas flow rates, because a larger oil/water volume ratio increases the interfacial area by giving a smaller diameter of the plume eye, the mass transfer parameter is higher. Furthermore, a large oil/water ratio decreases the starting gas flow rate for breaking the oil layer, increasing the mass transfer parameter. It was observed that k_wA is proportional to Q at flow rates below 4 l/min. With increasing oil volume ratio, the intermediate Regime II becomes narrower and finally too narrow to define. In the case for 4.5 l of oil, Regime III appears very abruptly at 5 l/min and shows the same dependence value of k_wA on Q as that in Regime I. In this flow rate regime, the thicker oil layer has more oil droplets

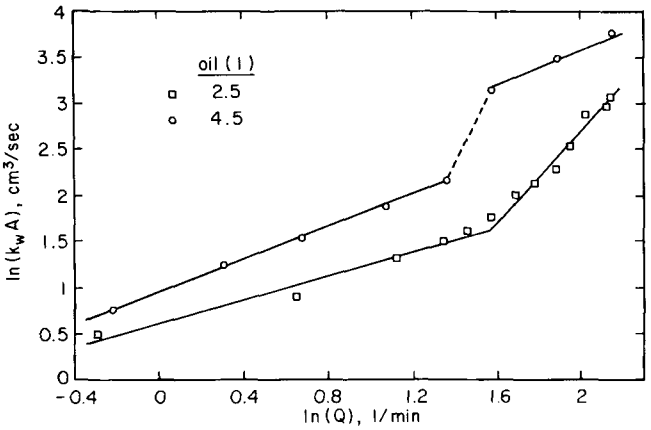

Fig. 7—Effect of oil volume on the mass transfer parameter for center tuyere injection.

separated from the oil layer in addition to the decreased diameter of a plume eye, which causes a higher value of k_wA than in the case of 2.5 l of oil. Some of the stirring energy due to the gas injection is consumed in producing turbulence at the interface between two immiscible phases and creating a circulation inside the upper oil phase, which can help break up the oil layer. Visual observation indicates that as the oil layer becomes thicker, the oil layer breaks into the droplets more easily due to the formation of more active and stronger circulation inside the oil layer. However, the critical gas flow rate for entraining the oil droplets does not change much. The mass transfer rate turns out to be very sensitive to the effect of oil volume fraction under the conditions tested, but the critical gas flow rate is only slightly dependent of the oil volume fraction.

Effect of Tuyere Diameter: The center tuyere diameter was reduced to 0.2 cm to investigate the effect of tuyere size on k_wA. The results are shown in Figure 8. No difference of k_wA is observed in the low flow rates (<6 l/min), but the larger size tuyere shows a slightly better two phase mass transfer in higher gas flow rates where violent entrainment of numerous oil droplets occurs. The apparent reason of this better mass transfer in higher flow rates is that as the tuyere diameter becomes larger, a greater number of large size bubbles reach the interphase region, which results in generating more turbulence of the interface between two phases.

Effect of Tuyere Position: The tuyere position was changed from a center to the vessel wall to investigate the

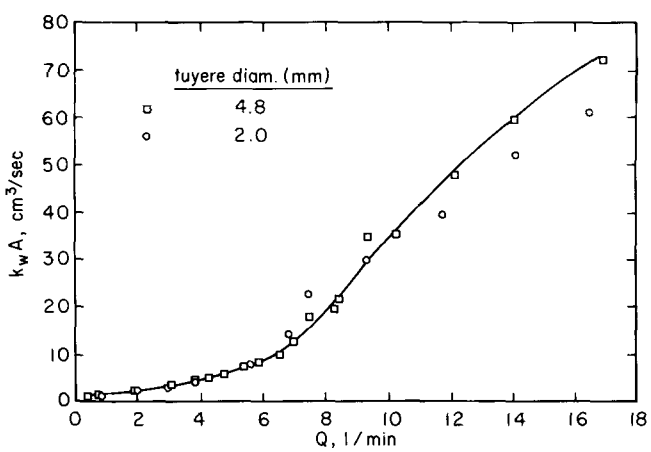

Fig. 8—Effect of tuyere size on the mass transfer parameter for center tuyere injection.

effect of tuyere location. The values of k_wA are plotted as a function of gas flow rate for the injection through a center, an off-center, and a side tuyere in Figure 9. For gas flow rates below 5 l/min, no difference in the values of k_wA for the three different tuyere arrangements was observed. However, above 5 l/min, a center tuyere arrangement gives faster two phase mass transfer than the other two offcenter tuyere arrangements. The apparent reason for this is shown schematically in Figure 10. In the case of an offcenter tuyere injection, the oil layer near the vessel wall on the opposite side of a tuyere is not affected much by the gas-liquid plume and the formation of oil droplets starts to appear at much higher gas flow rates, apparently because it requires more energy to break down the wider stagnant area of oil at the opposite side of the tuyere position. It was found that the mass transfer decreases significantly as the tuyere position moves from the center to the half distance of the bottom radius, while the mass transfer does not change wherever a tuyere locates between the half distance of the radius and the vessel wall. To investigate further the effect of tuyere position on the mass transfer, the number of tuyeres was varied. Figure 11 shows a plot of k_wA *vs* total flow rates for a center tuyere arrangement and the linear arrangements of two and three tuyeres. The same mass transfer rates were also observed in the region of low gas flow rates, but there are some differences between a center tuyere arrangement and linear arrangement of tuyeres at higher flow rates. As shown in Figure 10, these differences appear because the relatively narrow stagnant oil layers are formed near both the side walls across the centerline connecting tuyeres, where the movement of oil is not as active as in the case of a center tuyere injection. It was visually observed that these differences can be minimized by arranging the tuyeres in a concentric arrangement instead of a linear arrangement. The mass transfer at low gas flow rates is the same at a fixed total gas flow regardless of tuyere positions and numbers.

As shown in Figure 12, only two physical regimes of interaction between oil and water phase are observed over the flow rate range investigated in the offcenter tuyere arrangements and linear arrangements of tuyeres.

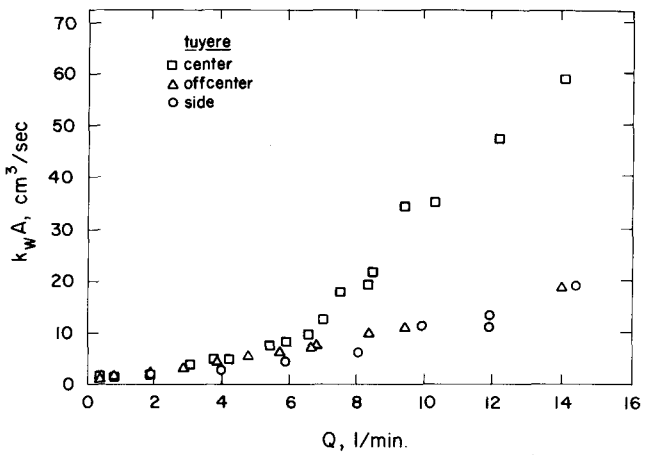

Fig. 9 — Effect of the position of a tuyere on the mass transfer parameter.

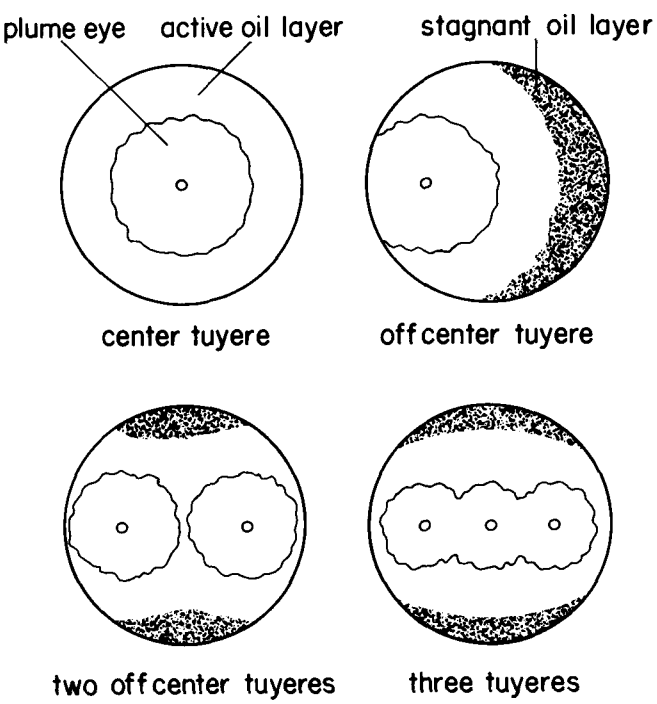

Fig. 10 — A schematic diagram of top views of oil layer during gas injection of high gas flow rates according to the different arrangements of tuyere(s).

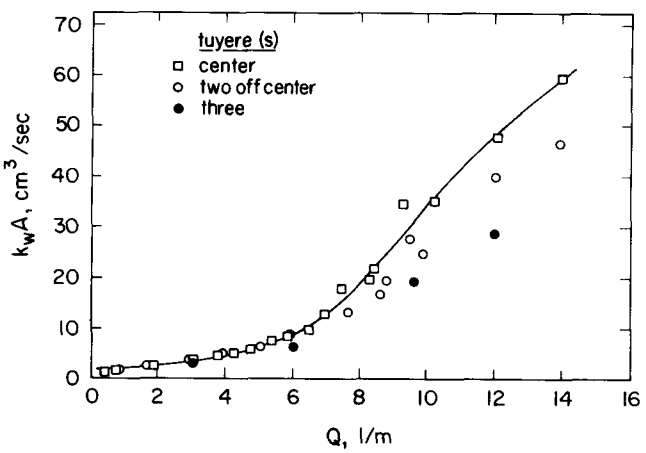

Fig. 11 — A plot of k_wA *vs* total gas flow rate for a center tuyere arrangement and linear arrangements of two and three tuyeres.

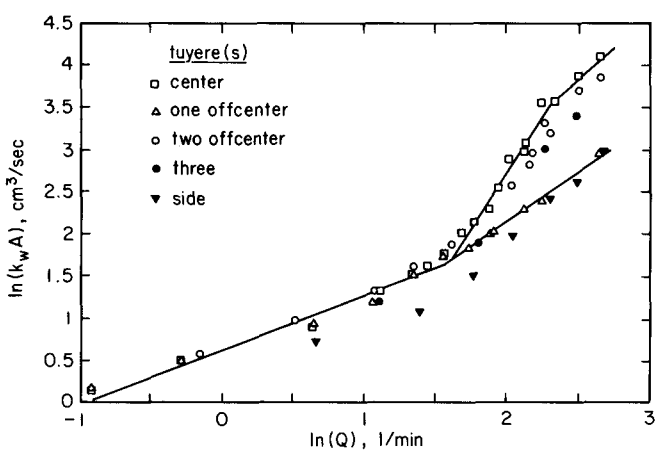

Fig. 12 — Relationship between k_wA and Q in terms of the order dependence, n, for 4 different tuyere patterns.

For off-center tuyere arrangements

$$k_w A \propto Q^{0.60} \quad (Q < 5 \text{ l/min})$$

$$k_w A \propto Q^{1.21} \quad (Q > 5 \text{ l/min})$$

For linear arrangements of tuyeres

$$k_w A \propto Q^{0.60} \quad (Q < 5 \text{ l/min})$$

$$k_w A \propto Q^{2.07} \quad (Q > 5 \text{ l/min})$$

Effect of Lance Injection: The mass transfer parameter was measured for gas injection through a model of a lance to determine if there are any differences between it and a bottom tuyere. Figure 13 shows a comparison of the mass transfer rate for gas injection through a lance with two side holes at the bottom center and a center tuyere. No difference in mass transfer rate was found in these two gas injection techniques. This observation shows that the two phase mass transfer is independent of the number of holes at the specified tuyere pattern and dependent only of the total gas flow rate.

To investigate further the effect of lance injection, the height of lance position in the vessel was varied. The Figure 13 also shows a plot of $\ln(k_w A)$ *vs* $\ln(Q)$ for lance injection at one-half bath depth. With the increase of lance depth into the bath, the mass transfer rate increases over the whole range of gas flow rates employed. The stirring energy of the injected gas for recirculation is sensitive to the lance position or depth as indicated by Eq. [19]. Therefore, the lower liquid mass transfer rate with shallower depth of the lance can be explained by less active turbulent behavior of oil/water interface due to the production of less stirring energy. This explanation is clearly proven in Figure 14 in which the data in Figure 13 are plotted in terms of stirring energy instead of flow rate. No difference of $k_w A$ was observed in the range of low energy, but higher values of $k_w A$ for a bottom position lance for higher energies were observed. As shown in Figure 14, only two physical regimes were found over the range of flow rates employed for lance injection in the middle of the bath.

In Regime I

$$k_w A \propto \varepsilon^{0.60}$$

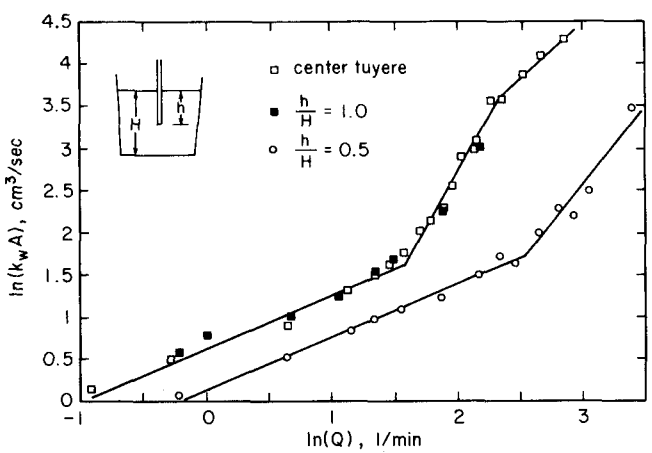

Fig. 13—A comparison between tuyere and lance injection, and effect of lance depth on the mass transfer parameter.

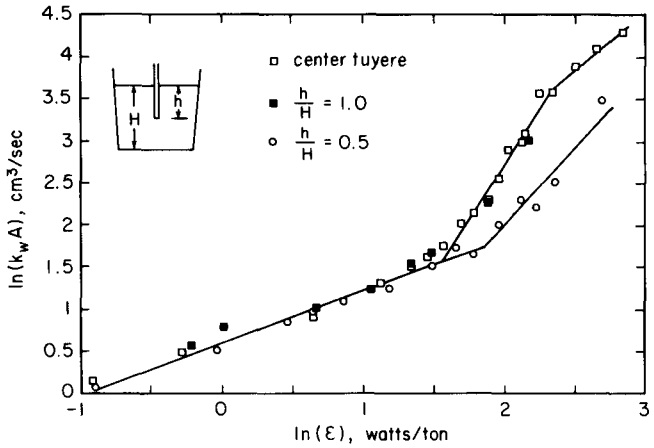

Fig. 14—A plot of $k_w A$ as a function of stirring energy density for two different depths of lance injection.

In Regime II

$$k_w A \propto \varepsilon^{1.92}$$

The reason for the presence of these two physical regimes is the same as that described earlier for tuyere positions.

C. *Estimation of the Mass Transfer Coefficient and Interfacial Area*

Experiments were conducted to measure the mass transfer coefficient of benzoic acid at the various positions in the solid/liquid system stirred by gas injection through the center tuyere. As the tuyere position comes closer to the center, more turbulence near the bath surface occurs. In the calculation of k_w using Eq. [18], it is further assumed that the bulk concentration of benzoic acid is equal to zero and the interface concentration is the same as the equilibrium concentration. The results in Figure 15 show that the mass transfer coefficient increases with increasing gas flow rates regardless of position of the sample over the gas flow rates tested. The highest mass transfer coefficient was observed in the region at the center of the surface layer (position 2). The mass transfer coefficient was found to be approximately proportional to $Q^{0.43}$. The value obtained in this study is relatively well consistent with the following correlation between k_l and gas flow rate for the mass transfer between two

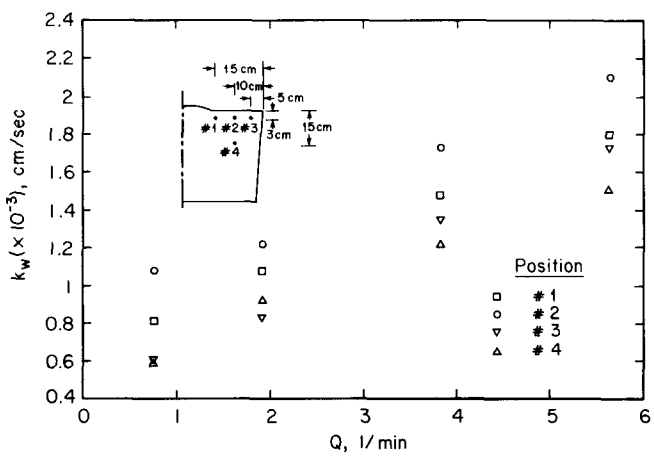

Fig. 15—A plot of mass transfer coefficient of benzoic acid as a function of flow rate at various positions in the ladle model.

immiscible liquids in a gas stirred reactor, which was experimentally determined by Richardson *et al.*[31]

$$k_1 = \beta\left(\frac{DQ}{A}\right)^{1/2}$$

where β is an experimentally determined coefficient. This correlation has provided a fairly good prediction for practical purposes.[32,33] However, this dependence value of k with respect to Q is higher that that (0.29) for graphite rod dissolution in a 6t argon stirred ladle using an offcentered porous plug near the ladle wall, as reported by Lehner.[26] This difference may be considered to be due to the different processes of gas injection, *i.e.*, location of injection.

The estimated interfacial area for the two phase mass transfer experiments and the planar interfacial area are shown in Figure 16. The estimated interfacial area was calculated from the k_wA of the liquid/liquid system and the average values of k_w determined from the dissolution of benzoic acid rod. The planar interfacial area decreases with flow rates because the plume eye decreases. The assumption is made that k_w is the same in both experiments because the values of diffusion coefficients of thymol and benzoic acid in water are nearly the same (6.8×10^{-6} and 8.4×10^{-6} cm^2/sec, respectively).[34] The estimated interfacial area is larger than the planar interfacial area even in the low flow rate range. The estimated interfacial area increases at a much greater rate at flow rates greater than about 4.5 l/min which corresponds to the formation of oil droplets which are entrained into the bath. Based on these results, it can be concluded that the abrupt change in the dependence of k_wA on flow rate is mainly due to the drastic increase of interfacial area between two phases.

IV. SUMMARY AND CONCLUSION

The rate controlling process in many metallurgical reactions in gas stirred ladles is mass transfer between metal and slag. The effect of operating variables was studied in the present work with a physical model. From the experimental results, it can be concluded that

1. The presence of a second phase (oil in the model, slag in the steelmaking ladle) increases mixing time significantly, indicating its resistance to the recirculatory velocity of fluid near the surface.
2. Better one phase mixing, as indicated by decreased mixing time, is observed as the position of a single tuyere moves from the center to the wall side of a vessel.
3. Three regimes of two phase mass transfer were observed in gas stirring through a center tuyere which are explained by the break-up of the oil into droplets and the entrainment of these droplets, causing an increase of the interfacial area. It is anticipated that a similar behavior occurs in slag/metal system.
4. Oil viscosity does not change the critical gas flow rate but affects the rate of two phase mass transfer to some extent in the higher flow rate region.
5. A large volume ratio of oil to water (slag to liquid metal) increases the rate of two phase mass transfer.
6. Mass transfer parameter for the offcenter tuyere arrangements does not increase with increasing gas flow rates as rapidly as the center and linear arrangements of tuyeres in the higher gas flow rate region. No difference is observed for the different tuyere arrangements in the lower flow rate region. Better mass transfer is expected for a concentric arrangement of tuyeres rather than for a linear arrangement.
7. The tuyere diameter does not significantly affect the rate of two phase mass transfer in the region of low gas flow rates.
8. The mass transfer rate for lance injection is independent of the number of holes and dependent only of the total gas flow rate and the lance position.
9. There is no difference in mass transfer rate for gas injection through a tuyere and lance injection at the same position. Lower mass transfer rate with shallower depth of a lance appears due to less stirring energy available.

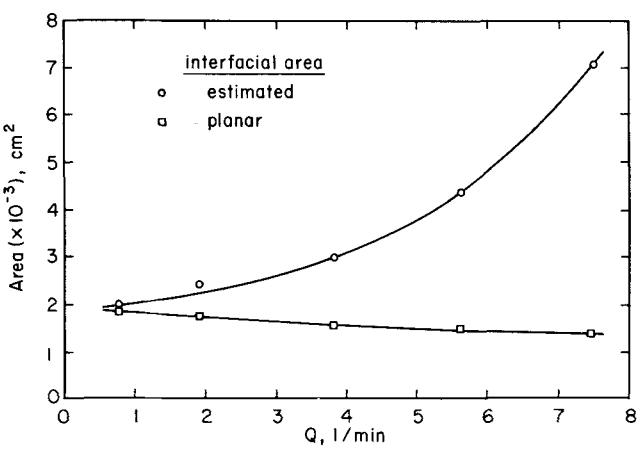

Fig. 16—A comparison between estimated and planar interfacial area for center tuyere injection.

For the relationship between mixing time and mass transfer rate, it is frequently mentioned in the literature that the mass transfer rate increases as mixing time decreases. Based on present results of mixing time and mass transfer experiments, this general assertion is found to be incorrect. For example, the mixing times for the offcenter tuyere arrangements are shorter than for a center tuyere, but two phase mass transfer is faster for a center tuyere. Therefore, the mixing time is not a good parameter in predicting the two phase mass transfer except when the same tuyere pattern is considered.

Based on the results of the physical modeling of a gas stirred ladle, information for the optimum conditions of inclusion removal and desulfurization in actual plant processes can be deduced. For obtaining low oxygen level in steel, it is necessary to prevent air contamination of steel during stirring, to promote the reaction between slag and metal, and to coalesce inclusions to slag by means of effective stirring without entraining slag deeply into the steel bath. In order to satisfy these criteria simultaneously, it is recommended to use lower flow rates of gas blowing for relatively long periods of time. The desulfurization process requires vigorous stirring which can maximize slag/metal mixing and penetration of slag into the steel. However, the process should be followed by a gentle stirring to remove any entrained slag from the melt.

NOMENCLATURE

A interfacial area (cm^2)
C concentration in bulk (gr/cm^3)

C' concentration at interface (gr/cm^3)
H depth of tuyere or lance position (cm)
J mass flux (gr/cm^3 sec)
K capacity coefficient of mass transfer, $k_l A/V_b$ (sec^{-1})
L depth of liquid bath (cm)
Q gas flow rate (l/min)
T temperature (K)
U_T linear velocity of gas at the tuyere outlet (cm/sec)
V volume (l)
W weight of rod (gr)
ΔW weight loss within a specified time (gr)
W_b weight of water (ton)
g gravity constant (gr/cm^2 sec)
h partition ratio
k mass transfer coefficient (cm/sec)
ρ density (gr/cm^3)
t time (min)
τ_m mixing time (sec)
ε stirring energy density (watts/ton)
λ geometrical scaling factor
μ viscosity (poise)
Δt time elapsed for dissolution (min)

subscripts

b bulk phase
d dispersed phase
i interface
g gas phase
l liquid phase
m metal phase
o oil phase
s slag phase
w water phase

superscript

° initial state

ACKNOWLEDGMENTS

The authors wish to thank R. I. L. Guthrie (McGill University) and R. Matway for helpful discussions, and M. Karvolois for performing the experiments with benzoic acid. The support of the research by the Center for Iron and Steelmaking Research and member companies, and N.S.F. grant (8421112) are acknowledged.

REFERENCES

1. J. Szekely, H. J. Wang, and K. M. Kiser: *Metall. Trans. B*, 1976, vol. 7B, pp. 287-95.
2. N. El-Kaddah and J. Szekely: *Scaninject I*, #3, MEFOS and Jernkontoret, June 1977, Luleå, Sweden.
3. T. DebRoy, A. K. Majumdar, and D. B. Spalding: *Appl. Math. Modelling*, 1978, vol. 2, pp. 146-50.
4. J. McKelliget, M. Cross, R. Gibson, and J. Brimacombe: *Heat and Mass Transfer in Metallurgical Systems*, D. B. Spalding and N. H. Afghan, eds., Hemisphere Pub. Co., New York, NY, 1981, pp. 349-72.
5. C. Aldham, N. Markatos, and M. Cross: *Proc. of Int. Conf. on Proc. Modelling*, Teesside Politechnic, Cleveland, U.K., May 1982.
6. R. I. L. Guthrie: *Iron and Steel Maker*, Jan. 1982, pp. 41-45.
7. Y. Sahai and R. I. L. Guthrie: *Metall. Trans. B*, 1982, vol. 13B, pp. 193-202.
8. Y. Sahai and R. I. L. Guthrie: *Metall. Trans. B*, 1982, vol. 13B, pp. 203-11.
9. S. Asai, M. Kawachi, and I. Muchi: *Scaninject III*, #12, MEFOS and Jernkontoret, June 1983, Luleå, Sweden.
10. M. Sano and K. Mori: *Trans. ISIJ*, 1983, vol. 23, pp. 169-75.
11. S. Asai, T. Okamoto, J. He, and I. Muchi: *Trans. ISIJ*, 1983, vol. 23, pp. 43-50.
12. R. Kaiyuan, Z. Aiqi, and Y. Shuqin: *Scaninject III*, #42, MEFOS and Jernkontoret, June 1983, Luleå, Sweden.
13. D. Mazumdar: Ph.D. Thesis, 1985, McGill Univ., Montreal, PQ, Canada.
14. O. Haida, T. Emi, S. Yamada, and F. Sudo: *Scaninject II*, #20, MEFOS and Jernkontoret, June 1980, Luleå, Sweden.
15. Q. Ying, L. Yun, and L. Liu: *Scaninject III*, #21, MEFOS and Jernkontoret, June 1983, Luleå, Sweden.
16. I. Sawada and T. Ohashi: *Tetsu-to-Hagané*, 1984, vol. 70, p. S161.
17. Y. Ohga, S. Taniguchi, and J. Kikuchi: *Tetsu-to-Hagané*, 1985, vol. 71, p. S897.
18. M. Hirasawa, K. Mori, M. Sano, Y. Shimada, and Y. Okazaki: *Tetsu-to-Hagané*, 1985, vol. 71, p. S898.
19. S. Endo and M. Hasegawa: *Tetsu-to-Hagané*, 1985, vol. 71, p. S899.
20. M. Ozawa, S. Nakayama, and T. Yajima: *Iron and Steel Maker*, Nov. 1984, pp. 22-23.
21. J. Ishida, K. Yamaguchi, S. Sugiura, N. Demukai, and A. Notoh: *Denki-Seiko*, 1981, vol. 52(1), pp. 2-8.
22. G. Carlsson, M. Bramming, and C. Wheeler: 5th International Iron and Steel Congress, April 6-9, 1986, Washington, DC.
23. K. Nakanishi, Y. Kato, T. Nozaki, and T. Emi: *Tetsu-to-Hagané*, 1980, vol. 66, pp. 1307-16.
24. R. Matway: unpublished work, Carnegie Mellon Univ., Pittsburgh, PA, 1986.
25. L. Heaslip, I. Sommervill, and W. Wilson: *Iron and Steel Maker*, Oct. 1985, pp. 37-39.
26. T. Lehner: Proc. Symp. "Ladle Treatment of Carbon Steel", McMaster Univ., Hamilton, ON, Canada, May 1979.
27. T. Hsiao, T. Lehner, and B. Kjellberg: *Scand. J. of Metallurgy*, 1980, vol. 9, pp. 105-10.
28. J. Billington and K. Gregory: *Radex-Rundschau*, Heft ½, 1981, pp. 368-73.
29. R. Calabrese, T. Chang, and P. Dang: *AIChE Journal*, 1986, vol. 32, No. 4, pp. 657-66.
30. C. Wang and R. Calabrese: *AIChE Journal*, 1986, vol. 32, No. 4, pp. 667-76.
31. F. Richardson, D. Robertson, and B. Staples: Proceedings of "The Darken Conference", U.S. Steel, Monroeville, PA, August 1976.
32. H. Gaye and J. Grosjean: Steelmaking Conf. AIME, March 1982, Pittsburgh, PA.
33. P. Riboud, J. Motte, D. Senaneuch, and M. Jeanneau: Symp. of "Ladle Treatment of Carbon Steel", McMaster Univ., Hamilton, ON, Canada, May 1979.
34. R. Reid, J. Prausnitz, and T. Sherwood: *The Properties of Gases and Liquids*, 3rd ed., McGraw-Hill Company, New York, NY, 1977.